

# ADAPTIVE HYSTERESIS CURRENT VECTOR CONTROL OF SYNCHRONOUS SERVO DRIVES WITH DIFFERENT TOLERANCE AREAS

István SCHMIDT, Katalin VINCZE, Károly VESZPRÉMI and Balázs SELLER

Department of Electrical Machines and Drives  
 Budapest University of Technology and Economics  
 H–1521 Budapest, Hungary  
 Phone: +36 1 463 3603  
 e-mail: veszi@eik.bme.hu

Received: June 29, 2000

## Abstract

Control methods of hysteresis current vector control of permanent magnet synchronous servo drive fed by voltage source inverter are examined. Detailed description of the control methods in stationary reference frame with circle, square and hexagon shape tolerance area using adaptive solutions is presented. The theoretical considerations are supported by simulation results.

*Keywords:* synchronous servo drive, current vector control, adaptive control, hysteresis control.

## 1. Introduction

The sinusoidal-field synchronous servo motor drive fed by a current regulated voltage source inverter is investigated. The assumptions about the motor are: the stator has symmetrical three-phase winding, the rotor is cylindrical, it has permanent magnet excitation with sinusoidal spatial distribution of the flux density. For the sake of simplicity  $L_d = L_q$  synchronous inductances and  $L'_d = L'_q = L_d$  subtransient inductances are assumed, the equivalent circuits in *Fig. 1* are used for the investigations, valid for transient processes also. The permanent magnet is represented by the pole-flux vector in the  $d$  direction with  $\Psi_p = \text{const.}$  magnitude and by the pole voltage vector in the  $q$  direction:

$$\bar{\psi}_p = \Psi_p e^{j\alpha}, \quad (1a)$$

$$\bar{u}_p = d\bar{\psi}_p/dt = jw\bar{\psi}_p, \quad (1b)$$

where  $\alpha$  is the angle of the rotor,  $w = d\alpha/dt$  is its angular speed. The torque of the motor in per-unit system is:

$$m = \Psi_p i \sin \vartheta_p = \Psi_p i_q, \quad (2)$$

where  $i$  is the magnitude of the  $\bar{i} = i e^{j\alpha_i} = i e^{j(\alpha+\vartheta_p)}$  current vector,  $\vartheta_p$  is the torque angle between the  $\bar{\psi}_p$  and  $\bar{i}$  vectors,  $i_q = i \sin \vartheta_p$  is the  $q$  component of the

current vector. In a synchronous servo drive the magnitude and the phase of the current vector are controlled. The reference current vector is:

$$\vec{i}_r = i_r e^{j\alpha_{ir}} = i_r e^{j(\alpha + \vartheta_{pr})}. \tag{3}$$

The vector diagram in Fig. 2 is drawn for one instant of the current control. The  $\vec{i}_r$  current reference vector rotates synchronously with the  $\vec{\psi}_p$  pole-flux vector. For positive  $m > 0$  torque the angle between them is  $90^\circ \leq \vartheta_{pr} < 180^\circ$ , for  $m < 0$  it is  $-180^\circ < \vartheta_{pr} \leq -90^\circ$ .

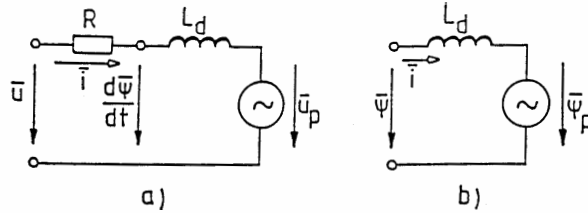


Fig. 1. The equivalent circuits of the synchronous servo motor: a., for voltages; b., for fluxes

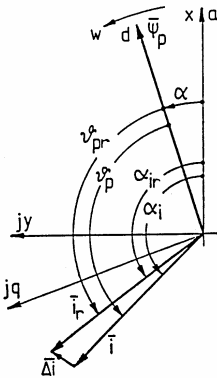


Fig. 2. Forming the current error vector

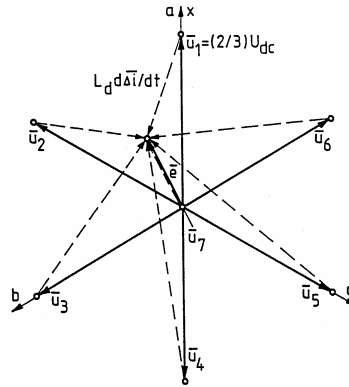


Fig. 3. The seven possible voltage vectors and  $L_d d\Delta\vec{i}/dt$

The current vector control oriented to the pole-field can be implemented by pulse width modulated (PWM) voltage-source inverter. It can provide 7 kinds of voltage vectors (Fig. 3):

$$k = 1 \dots 6 : \quad \vec{u}_k = (2/3)U_{dc} e^{j(k-1)\pi/3}, \quad k = 7 : \quad \vec{u}_k = 0. \tag{4}$$

The  $\bar{u}_7 = 0$  can be developed in two ways: either connecting all of the phases to the positive  $P$  side ( $7P$ ) or the negative  $N$  side ( $7N$ ). Investigating the seven kinds of voltage vector switchings, in the case of switching in one phase only (having single  $S = 1$  switching),  $\bar{u}$  is switched between two neighbour vectors ( $7P$  and  $7N$  are the neighbours of the vectors marked by  $k = 2, 4, 6$  and  $k = 1, 3, 5$ , respectively). If the switching is performed in two or three phases simultaneously (i.e. double  $S = 2$  or triple  $S = 3$  switching), further  $\bar{u}$  vectors are switched (e.g. at  $S = 3$  the vector in diagonal position).

The robust hysteresis current controllers determine the switching state of the inverter switching devices directly. The task of the PWM hysteresis current controller is to determine the instant of the evaluation and to perform the evaluation.

## 2. Hysteresis Current Vector Control

The operation of the analogue hysteresis current vector controllers is investigated in stationary and  $d - q$  reference frame, with current vector error tolerance area with different shape, but constant dimension. The operation in stationary reference frame is investigated in more detail.

### 2.1. Current Control in Stationary Reference Frame

The aim of hysteresis PWM current vector control is to keep the  $\bar{i}$  current vector in the tolerance area around the  $\bar{i}_r$  reference current vector. For the sake of simplicity this tolerance area can be a circle, a hexagon or a square. The flowchart of the hysteresis current vector control is presented in *Fig.4*. It detects when the  $\overline{\Delta i} = \bar{i}_r - \bar{i}$  current error vector reaches the border of the tolerance area; this is the  $t$  instant of the comparing. Then with an evaluation procedure based on a criterion it selects a voltage vector from the 7 possible ones and controls the inverter according to this. This is the instant of the intervention. The current control is adaptive, if the evaluation procedure considers also the state of the system (e.g. the  $\overline{\Delta i}' = \bar{i}_r' - \bar{i}'$  derivative of the current error vector), not only the  $\overline{\Delta i}$  current error vector.

To detect the instant of the comparing different values the  $\Delta i$  magnitude of the current error vector (with circle shape tolerance area), or  $\Delta i_x$  and  $\Delta i_y$  components (with circle or square shape tolerance area), or  $\Delta i_a = i_{ar} - i_a$ ,  $\Delta i_b = \Delta i_{br} - i_b$  and  $\Delta i_c = \Delta i_{cr} - i_c$  phase current errors (with hexagon shape tolerance area) can be used.

The derivative of the current error vector should be determined for the evaluation procedure. Substituting the  $\bar{i} = \bar{i}_r - \overline{\Delta i}$  expression to the voltage equation:

$$\bar{u} = R\bar{i} + L_d d\bar{i}/dt + \bar{u}_p, \quad (5)$$

it is:

$$\overline{\Delta i}' = d\overline{\Delta i}/dt = (\bar{e} - \bar{u})/L_d. \quad (6)$$

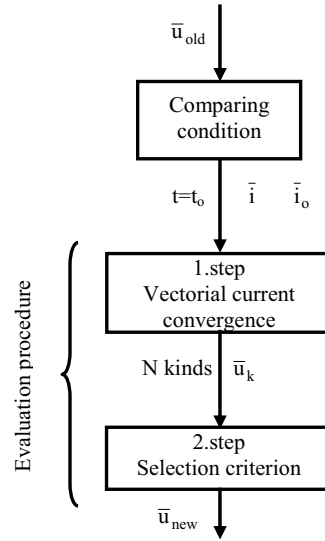


Fig. 4. The flowchart of the adaptive hysteresis current vector control

The derivative of the current error vector is determined by the state of the system ( $\bar{e}$ ) and the voltage  $\bar{u} = \bar{u}_k$  switched by the inverter. The system characteristic  $\bar{e} = R\bar{i} + L_d d\bar{i}_r/dt + \bar{u}_p$  voltage vector can be calculated by using the  $\bar{i}$  current, the  $\bar{i}_r$  reference current, the  $\bar{u}_p$  pole voltage and the  $R, L_d, \Psi_p$  machine parameters. This is the terminal voltage vector corresponding to the errorless  $\bar{i} = \bar{i}_r$  state. It is shown in Fig. 3 where the dashed lines are the  $L_d d\Delta\bar{i}/dt = \bar{e} - \bar{u}$  vectors corresponding to the seven possible  $\bar{u}_k$  voltage vectors.

### 2.1.1. Control by Circle Shape Tolerance Area

The  $t = t_0$  instant of the comparing is determined by reaching the tolerance circle with radius  $\Delta I$  by the  $\overline{\Delta i}(t_0) = \overline{\Delta i}_o = \Delta i_{ox} + j\Delta i_{oy}$  current error vector (Fig. 5a):

$$\Delta i_o = |\overline{\Delta i}_o| = \sqrt{\Delta i_{ox}^2 + \Delta i_{oy}^2} = \Delta I. \quad (7)$$

At the comparing instant the magnitude of the current error vector is constant ( $\Delta i_o = \Delta I = \text{const.}$ ), the phase current errors are different but they are inside the  $\pm\Delta I$  range.

It can be proved geometrically that those  $\bar{u}_k$  voltage vectors move the  $\overline{\Delta i}$  back into the tolerance circle, which result in  $\overline{\Delta i}'_{ko}$  current error vector derivative at  $\overline{\Delta i}_o$ , which results in negative scalar product with the current error vector:

$$F_{ko} = \overline{\Delta i}_o \cdot \overline{\Delta i}'_{ko} = \overline{\Delta i}_o \cdot (\bar{e}_o - \bar{u}_k)/L_d < 0 \quad (8)$$

$(\overline{\Delta i'_{ko}} = \overline{\Delta i'}(\bar{u} = \bar{u}_k, t = t_o), \bar{e}_o = \bar{e}(t_o))$ . The symbol ‘ $\cdot$ ’ means scalar product. This is the vectorial convergence criterion for circle shape tolerance area. If it is satisfied at every switching, the  $\overline{\Delta i}$  current error vector always remains in the tolerance circle.

The adaptive evaluation is done by the following two steps (see *Fig.4*):

- *First* the above determined current convergence condition is used to select those  $N$   $\bar{u}_k$  voltage vectors from the possible seven, which move the  $\overline{\Delta i}$  back into the tolerance circle. By applying these  $\bar{u}_k$  vectors the  $\overline{\Delta i} = \overline{\Delta i}_k$  current vector remains inside the tolerance circle for  $T_k$  time interval. Using linear approximation for the  $t_o \leq t \leq t_o + T_k$  time interval:

$$\overline{\Delta i}_k = \overline{\Delta i}_o + (t - t_o)\overline{\Delta i'_{ko}}. \quad (9)$$

At the next comparing at  $t_o + T_k$  instant the current error vector is on the tolerance circle again  $\overline{\Delta i}_k(t_o + T_k) = \overline{\Delta i}_{k1}$ :

$$|\overline{\Delta i}_{k1}| = |\overline{\Delta i}_o + \overline{\Delta i'_{ko}}T_k| = \Delta I, \quad (10)$$

$$T_k = -2F_{ko} / |\overline{\Delta i'_{ko}}|. \quad (11)$$

- As the *second* step one should be selected from the  $N$  possible voltage vectors. The selection criterion can be determined by many different concepts. Some of them are listed here:

**C1. The strongest intervention:** If the selection of  $\bar{u}_k$  is based on the magnitude of the  $\overline{\Delta i}_o \cdot \overline{\Delta i'_{ko}}$  scalar product, then the most negative scalar product results in the strongest intervention.

**C2. The lightest intervention:** The selection of the least negative  $\overline{\Delta i}_o \cdot \overline{\Delta i'_{ko}}$  results in the lightest intervention.

**C3. Intervention resulting in the longest switching pause:** In this case that  $\bar{u}_k$  is selected for which  $\overline{\Delta i}_k$  remains inside the tolerance circle for the longest time:

$$\max(T_k). \quad (12)$$

It means that the  $f_v = 1/T_k$  vector changing frequency is minimal in this case.

**C4. Intervention resulting in the smallest switching frequency:** In this case that  $\bar{u}_k$  is selected for which the  $T_k/S_k$  time is maximal, the switching frequency of the transistors is minimal:

$$\min(f_e) = \min(S_k/T_k), \quad (13)$$

where  $f_e$  is the resultant switching frequency of the transistors and  $S_k = 1, 2, 3$  considers whether single, double or triple switching is necessary.

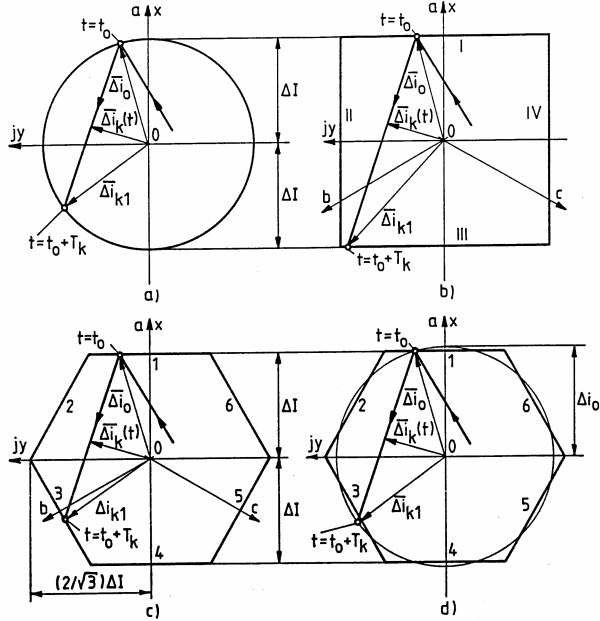


Fig. 5. Circle (a), rectangle (b), hexagon (c) and combined (d) shape tolerance area

### 2.1.2. Control by Square Shape Tolerance Area

The  $t_o$  instant of the comparing is determined by reaching the tolerance square with side  $2\Delta I$  by  $\overline{\Delta i}_o$  (Fig. 5b). The current error vector components on the different sides are:

$$\begin{aligned}
 \text{Side I.:} \quad \Delta i_{ox} = \Delta i_{oa} = \Delta I, \quad \text{Side II.:} \quad \Delta i_{oy} = (\Delta i_{ob} - \Delta i_{oc}) / \sqrt{3} = \Delta I, \\
 \text{Side III.:} \quad \Delta i_{ox} = \Delta i_{oa} = -\Delta I, \quad \text{Side IV.:} \quad \Delta i_{oy} = (\Delta i_{ob} - \Delta i_{oc}) / \sqrt{3} = -\Delta I.
 \end{aligned} \tag{14}$$

The current error vector at the comparing is in the range of  $\Delta I \leq \Delta i_o \leq \sqrt{2}\Delta I$ . The absolute value of the phase current errors can be maximum  $|\Delta i_{oa}|_{\max} = \Delta I$ ,  $|\Delta i_{ob}|_{\max} = |\Delta i_{oc}|_{\max} = \sqrt{2}\Delta I \cos 15^\circ \approx 1.366\Delta I$ .

In this case the vectorial convergence criterion depends on the fact which side of the square is reached by  $\overline{\Delta i}$ . The conditions to move the  $\overline{\Delta i} = \overline{\Delta i}_k$  back to the tolerance square by the applied  $\overline{u}_k$  voltage are the following:

$$\begin{aligned}
 \text{on side I.:} \quad \Delta i'_{kox} < 0, \quad \text{on side II.:} \quad \Delta i'_{koy} < 0, \\
 \text{on side III.:} \quad \Delta i'_{kox} > 0, \quad \text{on side IV.:} \quad \Delta i'_{koy} > 0.
 \end{aligned} \tag{15}$$

Inside the tolerance area the linear approximation (9) is used again, expressing by  $x - y$  components:

$$\Delta i_{kx} = \Delta i_{ox} + \Delta i'_{kox}(t - t_o), \quad \Delta i_{ky} = \Delta i_{oy} + \Delta i'_{koy}(t - t_o). \quad (16)$$

It can be proved that applying  $\bar{u}_k$  voltage vector the developed  $\overline{\Delta i}_k$  current error vector reaches the lines of the sides I., II., III. and IV after the following time intervals:

$$\begin{aligned} T_{kI} &= (\Delta I - \Delta i_{ox}) / \Delta i'_{kox}, & T_{kII} &= (\Delta I - \Delta i_{oy}) / \Delta i'_{koy}, \\ T_{kIII} &= (-\Delta I - \Delta i_{ox}) / \Delta i'_{kox}, & T_{kIV} &= (-\Delta I - \Delta i_{oy}) / \Delta i'_{koy}. \end{aligned} \quad (17)$$

The minimum of these values  $T_k = \min(T_{ki} > 0)$  determines the  $t_o + T_k$  instant of the next comparing corresponding to  $\bar{u}_k$ , when  $\overline{\Delta i}_k(t_o + T_k)$  is again on the side of the tolerance square.

The evaluation is done by two steps again:

- *First* those  $N$   $\bar{u}_k$  voltage vectors are selected from the possible seven that satisfy the current convergence condition (15), i.e. move the  $\overline{\Delta i}$  back into the tolerance square.
- As the *second* step, knowing  $T_k$  and  $S_k$  one should be selected from the  $N$  possible voltage vectors using a selection criterion. The selection criteria can be the same as in section 2.1.

### 2.1.3. Control by Hexagon Shape Tolerance Area

The  $t_o$  instant of the comparing is determined by reaching the tolerance hexagon with side distance  $2\Delta I$  by  $\overline{\Delta i}_o$  (Fig. 5c). The current error vector components on the different sides are:

$$\begin{aligned} \text{Side 1.: } \Delta i_a &= \Delta I, & \text{Side 4.: } \Delta i_a &= -\Delta I, \\ \text{Side 2.: } \Delta i_c &= -\Delta I, & \text{Side 5.: } \Delta i_c &= \Delta I, \\ \text{Side 3.: } \Delta i_b &= \Delta I, & \text{Side 6.: } \Delta i_b &= -\Delta I. \end{aligned} \quad (18)$$

The current error vector at the comparing is in the range of  $\Delta I \leq \Delta i_b \leq (2/\sqrt{3}) \Delta I$ . The absolute value of the phase current errors can be maximum  $\pm \Delta I$ .

In this case the vectorial convergence criterion depends on the fact which side of the hexagon is reached by  $\overline{\Delta i}$ . The conditions to move the  $\overline{\Delta i} = \overline{\Delta i}_k$  back to the tolerance hexagon by the applied  $\bar{u}_k$  voltage are the following:

$$\begin{aligned} \text{on side 1.: } \Delta i'_{kox} &< 0, & \text{on side 4.: } \Delta i'_{kox} &> 0, \\ \text{on side 2.: } \Delta i'_{kox} &< -\sqrt{3}\Delta i'_{koy}, & \text{on side 5.: } \Delta i'_{kox} &> -\sqrt{3}\Delta i'_{koy}, \\ \text{on side 3.: } \Delta i'_{kox} &> \sqrt{3}\Delta i'_{koy}, & \text{on side 6.: } \Delta i'_{kox} &< \sqrt{3}\Delta i'_{koy}. \end{aligned} \quad (19)$$

It can be proved that applying  $\bar{u}_k$  voltage vector the developed  $\overline{\Delta i}_k$  current error vector reaches the lines of the sides 1, 2, 3, 4, 5 and 6 after the following time intervals:

$$\begin{aligned}
 T_{k1} &= (\Delta I - \Delta i_{ox}) / \Delta i'_{kox}, & T_{k4} &= (-\Delta I - \Delta i_{ox}) / \Delta i'_{kox}, \\
 T_{k2} &= \frac{2\Delta I - \Delta i_{ox} - \sqrt{3}\Delta i_{oy}}{\Delta i'_{kox} + \sqrt{3}\Delta i'_{koy}}, & T_{k5} &= \frac{-2\Delta I - \Delta i_{ox} - \sqrt{3}\Delta i_{oy}}{\Delta i'_{kox} + \sqrt{3}\Delta i'_{koy}}, \\
 T_{k3} &= \frac{-2\Delta I - \Delta i_{ox} + \sqrt{3}\Delta i_{oy}}{\Delta i'_{kox} - \sqrt{3}\Delta i'_{koy}}, & T_{k6} &= \frac{2\Delta I - \Delta i_{ox} + \sqrt{3}\Delta i_{oy}}{\Delta i'_{kox} - \sqrt{3}\Delta i'_{koy}}. \quad (20)
 \end{aligned}$$

The minimum of these values  $T_k = \min(T_{ki} > 0)$  determines the  $t_o + T_k$  instant of the next comparing corresponding to  $\bar{u}_k$ , when  $\overline{\Delta i}_k(t_o + T_k)$  is again on the side of the tolerance hexagon.

The two steps of the evaluation are similar to the previous procedures.

The current vector controls discussed so far are adaptive, since the evaluation procedures consider the derivative of the current error besides the current error. By hexagon shape tolerance area the evaluation can be based on the current error only. In this case the one-step evaluation procedure switches the phase  $a$  to the positive side if  $\Delta i_a > \Delta I$ , and to the negative side if  $\Delta i_a < \Delta I$  (the operation is similar in phase  $b$  and  $c$  also). This simple method is the (phase-by-phase) bang-bang control. In this case the vectorial convergence condition (19) is not satisfied at every switching, that is why  $\pm 2\Delta I$  phase current error can be generated. This current control is susceptible to high frequency limit cycle at low speed.

#### 2.1.4. Control by Combined Tolerance Area

It can be established from the previous discussion that the  $t_c$  comparing instant can be determined most easily at the hexagon shape tolerance area (18). On the other hand, the  $T_k$  time corresponding to the  $\bar{u}_k$  voltage vectors satisfying the vectorial current convergence criterion can be calculated most easily with the circle shape tolerance area (11). That is why it is worth combining these two tolerance area methods. The combined tolerance area method is demonstrated in Fig. 5d. The comparing is performed using the  $2\Delta I$  side distance hexagon, while the evaluation is based on the circle shape tolerance area.  $T_k$  can be calculated by (11), using  $\Delta i_o$  in (10) (changing in a small range only) instead of  $\Delta I$ . The resultant current vector control is approximately equivalent to a circle shape tolerance area current control operating with a  $\Delta i_o$  changing radius circle tolerance area (changing between  $\Delta I$  and  $(2/\sqrt{3})\Delta I$ ), but the comparing is performed if the  $2\Delta I$  side distance hexagon not the circle is reached (e.g. Fig. 5d, side 3.). In this way the phase current errors remain in the  $\pm\Delta I$  range.



## 2.2. Current Control in $d$ - $q$ Reference Frame

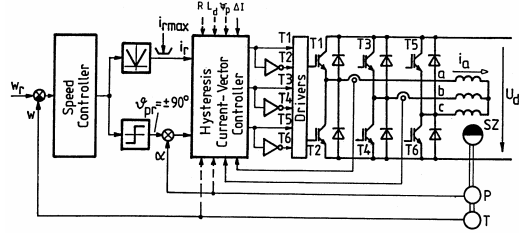


Fig. 6. The implementation of the current control

In this case the aim of hysteresis current vector control is to keep the  $\bar{i}^*$  current vector in the tolerance area around the  $\bar{i}_r^*$  reference current vector. (The superscript \* refers to the  $d - q$  reference frame, and e.g.  $\bar{i}^* = \bar{i}e^{-j\alpha}$ . The tolerance area is set in stationary reference frame so far. The circle and square shape tolerance area can be used in  $d - q$  reference frame also. However the evaluating Eqs. (5,6) must be used in  $d - q$  reference frame:

$$\bar{u}^* = R\bar{i}^* + L_d d\bar{i}^*/dt + j\omega L_d \bar{i}^* + \bar{u}_p^*, \quad (21)$$

$$\overline{\Delta i}^{*'} = d\overline{\Delta i}^*/dt = (\bar{f} - \bar{u}^*)/L_d, \quad (22)$$

where  $\bar{f} = R\bar{i}^* + L_d d\bar{i}^*/dt + j\omega L_d \bar{i}^* + \bar{u}_p^* = \bar{e}^* - j\omega L_d \overline{\Delta i}^{*}$  is a system-state dependent vector. Making the calculations according to sections 2.1.1. and 2.1.2. but using the above equations in  $d - q$  reference frame by \*  $d - q$  quantities, the results got are similar to those of the stationary case. Even using the circle shape tolerance area the result is the same.

## 3. Simulation Results

### 3.1. Simulation Method

The simulation model of the permanent magnet synchronous machine is derived from the vectorial equation (6) (resulting two electrical equations for the  $x - y$  components) extending it by the two mechanical differential equations:

$$di_x/dt = (u_{kx} - u_{px} - Ri_x) / L_d, \quad (23)$$

$$di_y/dt = (u_{ky} - u_{py} - Ri_y) / L_d, \quad (24)$$

$$dw/dt = (m - m_\ell)T_{st}, \quad (25)$$

$$d\alpha/dt = w, \quad (26)$$

where  $m_\ell$  is the load torque and  $T_{st}$  is the nominal starting time. The per-unit system is used for the simulation. The sensors, the control circuits and the voltage source inverter are assumed to be ideal. The non-linear differential equation system is solved numerically. The comparing instant at the tolerance band is determined by iteration.

### 3.2. Simulation Results

The block diagram of the considered controlled drive is presented in *Fig. 6*. The connections and parameters with dashed lines are necessary for the hysteresis current vector controller only for adaptive control, to calculate the  $\overline{\Delta i}' = \bar{i}'_r - \bar{i}'$  derivative of the current error vector. The simulated process is a speed regulated starting and the following quasi steady-state operating. The  $i_r$  magnitude of current vector reference signal of the subordinated current control loop (3) is provided by the PI speed controller, limiting it by  $i_r \leq i_{r \max}$  (*Fig. 6*). The reference of the torque angle is constant:  $\vartheta_{pr} = 90^\circ = \text{const}$ . The following parameters are used:  $R = 0.02$ ;  $L_d = 0.2$ ;  $\Psi_p = 1$ ;  $T_{st} = 31.4$ ;  $U_{dc} = 4$ ;  $m_\ell = 0.5$ ;  $i_{r \max} = 3$  (current limit);  $\Delta I = 0.1$ ;  $W_n = 314/\text{s}$  (nominal angular speed);  $W_r = 1$  (speed reference).

The investigated process contains a starting period  $T_s$  and the following steady-state period  $T_{ss}$  with  $W = 1$  speed. For the whole process ( $W_n t = 40 = T$ ) the torque, the speed and the phase currents are shown in *Fig. 7*. Circle shape tolerance area is used. These time functions are practically the same with hexagon and combined tolerance area. The starting and the steady-state part of the process are marked, both take  $T_s = T_{ss} = T/2 = 20$  pu. time.

The adaptive current controls using a circle, hexagon and combined tolerance area are investigated considering the number of switching for the starting and steady-state period of the process. The evaluation is performed using the C3 criterion resulting in the longest switching pause. The  $\bar{u}_k = \bar{u}_7 = 0$  voltage vector is developed by single switching always ( $S_k = 1$ ). The simple (not adaptive) bang-bang current control is investigated too.

The simulation results are presented in *Table 1* for the starting period, in *Table 2* for the steady-state part.  $N_a, N_b, N_c$  are the numbers of switching in phase  $a, b$  and  $c$ , respectively.  $N_1, N_2, N_3$  are the numbers of the single, the double and the triple switchings, respectively.  $N = N_a + N_b + N_c = N_1 + 2N_2 + 3N_3$  is the resultant number of switching. The number of comparing (voltage vector changing) can be calculated as  $N_v = N_1 + N_2 + N_3$ . The average switching frequency of the transistors can be calculated, e.g. for phase  $a$ :

$$f_{ka} = N_a W_n / (2\Delta T), \quad (27)$$

where  $N_a$  is the number of switching in phase  $a$  during time interval  $\Delta T$ . As an example: according to *Table 2* in the steady-state part in phase  $a$  with circle shape tolerance area adaptive current control:  $N_a = 414$ ;  $\Delta T = T_{ss} = 20$ ; so  $f_{ka} = 414 \cdot 314 / (2 \cdot 20) \approx 3252$  Hz.

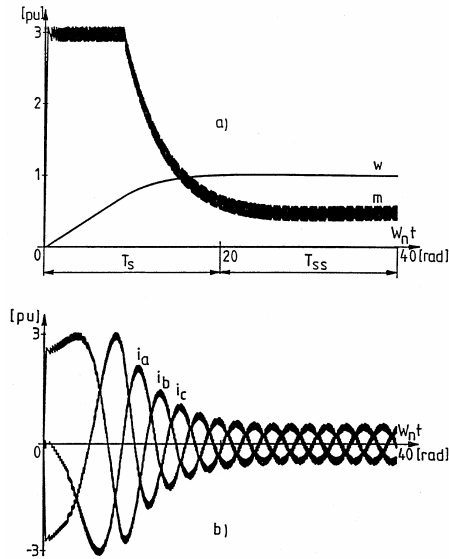


Fig. 7. The speed, torque (a) and the phase currents (b) for the examined process

Table 1. Statistics of the starting process

Methods	$N_a$	$N_b$	$N_c$	$N$	$N_1$	$N_2$	$N_3$	$N_v$
Circle	316	303	316	935	422	255	1	678
Hexagon	318	322	283	923	425	249	0	674
Combined	316	290	283	889	415	232	2	653
Bang-Bang	337	320	330	987	987	0	0	987

Table 2. Statistics of the steady-state operation

Methods	$N_a$	$N_b$	$N_c$	$N$	$N_1$	$N_2$	$N_3$	$N_v$
Circle	414	452	433	1299	457	421	0	878
Hexagon	406	436	424	1266	425	419	1	845
Combined	366	393	416	1175	486	340	3	829
Bang-Bang	313	347	324	984	984	0	0	984

It can be established from the *Tables* that there is no significant difference in the switching number comparing the three adaptive hysteresis current control methods. The simple bang-bang current control generates more switching during starting (caused by the limit-cycles), and less switching at steady-state, comparing

with the adaptive methods. There is an evaluation criterion for the adaptive controls which results in less switchings than the bang-bang control in steady-state [6].

#### 4. Conclusions

The examined three adaptive methods are practically identical in controlling respect. The switching numbers for the examined three methods are practically the same. The real-time microcomputer implementation of the combined method is more simple (comparing conditions, determination of  $T_k$  time until the next comparing). Even this method results in less switching number. Considering these advantages, the combined method is preferred.

The advantage of each adaptive method against the bang-bang control is that the current error is always inside the tolerance area and no limit cycle is generated.

#### Acknowledgement

This paper was supported by the Hungarian N.Sc. Fund (OTKA No. T023816 and T032207) for which the authors express their sincere gratitude.

#### References

- [1] BORD, D. M. – NOVOTNY, D. W., Current Control of VSI-PWM Inverters, *IEEE Trans. Industry Applications*, **21** No. 4 (1985), pp. 562–570.
- [2] NABAE, A. – OGASAWARA, S. – AKAGI, H., A Novel Control Scheme of Current-Controlled PWM Inverters, *IEEE-IAS Conf. Rec.*, (1985), pp. 473–478.
- [3] NAGY, I., Novel Adaptive Tolerance Band Based PWM for Field-Oriented Control of Induction Machines, *IEEE Trans. Ind. Electronics*, **41** No. 4 (1994), pp. 406–417.
- [4] KNOW, B. H. – KIM, T. W. – YOUM, J. H., A Novel SVM-Based Hysteresis Current Controller, *IEEE Trans. Power Electronics*, **13** No. 2 (1998), pp. 297–307.
- [5] KAZMIERKOWSKI, M. P. – MALESCANI, L., Current Control Techniques for Three-Phase Voltage-Source PWM Converters: a Survey, *IEEE Trans. Ind. Electronics*, **45** No. 5 (1998), pp. 691–703.
- [6] SCHMIDT, I. – VINCZE, K. – VESZPRÉMI, K., Adaptive Hysteresis Current Vector Controls of Synchronous Servo Drives, *Electromotion*, **6** No. 1–2 (1999), pp. 19–24.